J. Chem. Sci. Vol. 128, No. 4, April 2016, pp. 671–679.
DOI 10.1007/s12039-016-1060-x

Silane@TiO_2 nanoparticles-driven expeditious synthesis of biologically active benzo[4,5]imidazo[1,2-a]chromeno[4,3-d]pyrimidin-6-one scaffolds: A green approach

VILAS N MAHIRE[a], VIJAY E PATEL[b], ASHOK B CHAUDHARI[a], VIKAS V GITE[a] and PRAMOD P MAHULIKAR[a,*]

[a]School of Chemical Sciences, North Maharashtra University, Jalgaon, Maharashtra, India
[b]School of Life Sciences, North Maharashtra University, Jalgaon, Maharashtra, India
e-mail: mahulikarpp@rediffmail.com

MS received 30 December 2015; revised 5 February 2016; accepted 17 February 2016

Abstract. A simple, efficient and environmentally benign protocol has been developed for the synthesis of substituted benzo[4,5]imidazo[1,2-a]chromeno[4,3-d]pyrimidin-6-one by a reaction of 4-hydroxycoumarin, aldehydes and 2-aminobenzimidazole using silane@TiO_2 nanoparticles as heterogeneous catalyst under reflux condition in ethanol. The surface modification of TiO_2 nanoparticles was confirmed by using FT-IR, FE-SEM, EDX, XRD and TEM analyses. Furthermore, the stability of the catalyst was evaluated by thermal gravimetric analysis (TGA). Some advantages of this method are high yield of products, short reaction time; recyclability of the catalyst and column chromatography-free protocol. The synthesized compounds were screened for their *in vitro* antioxidant activity and most of the compounds exhibited remarkable antioxidant activity.

Keywords. 2-aminobenzimidazole; 4-hydroxycoumarin, aldehydes; silane@TiO_2 nanoparticles; benzo[4,5]imidazo[1,2-a]chromeno[4,3-d]pyrimidin-6-one.

1. Introduction

In recent years, nano-catalysis has been utilized as an alternative approach for the improvement in rates, yields and workability of many significant organic reactions. This also leads to a search for or design of new efficient affordable catalysts for specific applications in synthetic chemistry.[1] Nanoparticles have large surface area and due to this they get strongly agglomerated and hence their surface modification is an alternative way to produce new hybrid nanoparticles having virtuous properties.[2,3] The covalent attachment of functionalities on to the surface of nanoparticles enhances their newer properties which either increases the interaction or decrease the aggregation of nanoparticles which lead to various purposes to wider applications.[4–7] Nano materials have wide applications in science and technology such as medicinal, cosmetics and environmental purification, etc. Titanium dioxide belongs to the family of transition metal oxides and is considered as an ideal photocatalyst because of its merits such as low cost, nontoxicity, high stability, optical and electronic properties, etc. Furthermore, its band gap is sufficient to initiate a variety of organic reactions.[8,9]

Multi-component reactions are becoming the most significant synthetic tool for synthesis and design of new libraries of molecules of pharmaceutical interest through single step reactions.[10–12] In modern organic synthesis, combination of green chemistry and multi-component reactions will lead to generation of molecules with structural complexity in a single step from three or more reactants with greater efficiency and atom economy.[13–16] Therefore, the design of efficient multi-component reactions offers an enduring challenge for synthetic organic chemists.

In the development of several new drugs, the fused heterocyclic scaffolds with nitrogen and oxygen atoms play an important role in medicinal chemistry. Benzimidazole derivatives are important pharmacophores and considered as privileged structures in medicinal chemistry.[17,18] Benzimidazole derivatives have been reported to possess diverse biological activities such as antihistamine, antitumor, antibacterial, antifungal and antioxidant,[19] etc. Various substituted benzimidazoles are known to have diverse biological activities and among them 2-substituted benzimidazoles are found to be more potent.[20] Furthermore, the chromene[2,3-d]pyrimidine derivatives occupy an important place in the realm of natural and synthetic organic chemistry because of their biological and pharmacological activities

*For correspondence

such as antioxidant, antimicrobial,[21] antitumor,[22] antitubercular,[23] analgesic,[24] inflammatory,[25] etc.

To the best of our knowledge only Heravi *et al*., and Mazhukina *et al*., have reported the synthesis of benzo[4,5]imidazo[1,2-a]chromeno[4,3-d]pyrimidin-6-one derivatives.[26] However, there are no other reports on the synthesis of these benzo[4,5]imidazo[1,2-a] chromeno[4,3-d]pyrimidin-6-ones. This inspired us to continue our work on the multi-component synthesis under environmentally benign approach. In this article, we wish to report the synthesis of benzo[4,5] imidazo[1,2-a]chromeno[4,3-d]pyrimidin-6-one derivatives by a reaction of 4-hydroxycoumarin (**1**) with aromatic aldehydes (**2a-q**) and 2-aminobenzimidazole (**3**), in the presence of catalytic amount of silane@TiO_2 nanoparticles as an efficient catalyst (scheme 2). All synthesized compounds were screened for their antioxidant activities and it was found that most of the compounds exhibit excellent antioxidant properties.

2. Experimental

2.1 *Material and Methods*

All chemicals purchased from Sigma-Aldrich and S. D. Fine chemicals Ltd. were used without further purification. All solvents and chemicals obtained from S. D. fine chemicals used were of reagent grade. Melting points of all synthesized compounds were taken in open capillary tubes and are uncorrected. Reactions were monitored by thin-layer chromatography (TLC) on 0.2 mm precoated silica-gel 60 F254 plates (E. Merck). The spots were detected under UV light. The IR spectra (KBr) were recorded on Shimadzu IR Affinity-1 FT-IR spectrophotometer. The ^{1}H NMR and ^{13}C NMR spectra were recorded on a FT-NMR Cryo-magnet Bruker Avance-II spectrometer at 400 and 100 MHz, respectively, using DMSO-d_6 as solvent and the chemical shift values are recorded on the δ scale and coupling constant (J) values are in hertz (Hz). Mass spectra were recorded on Waters, Q-Tof Micromass (LCMS) spectrometer. TGA data were obtained with Perkin Elmer instrument at the temperature range of 28–800°C at a constant heating rate of 10°C/min in the nitrogen atmosphere (20 mL/min). X-ray diffractograms (XRD) of the catalyst were recorded in the range of 10–80° on a Bruker X-ray diffractometer with Ni-filtered Cu Kα radiation at a wavelength of 1.54060 Å. The FE-SEM analysis of the catalyst was performed on a Hitachi S-4800 scanning electron microscope (Japan) with accelerating voltage of 30 KV. The EDX analysis of the catalyst was performed by using Bruker EDX flash detector mode 5030. The Transmission Electron Microscopy of the catalyst was performed on PHILIPS CM200 of operating voltages of 20–200 kV, Resolution 2.4 Å. DPPH radical scavenging assay was performed on Shimadzu UV mini-1240 UV-Vis Spectrophotometer.

2.2 *Preparation of Silane@TiO_2 nanoparticles*

The TiO_2 nanoparticles were synthesized by sol-gel method[27] and then treated for surface modification. The surface modification of TiO_2 was achieved by reacting TiO_2 nanoparticles with vinyltriethoxysilane.[28] Typically, TiO_2 nanoparticles (1 g) were dispersed in acetone (10 mL) and the mixture was sonicated for 5–6 min. Simultaneously, vinyltriethoxysilane (0.5 mL) solution was prepared in acetone (10 mL) and then added slowly into TiO_2 solution under vigorous stirring provided by a high speed disperser and the mixture was stirred for an additional 20 min. After the modification of TiO_2, acetone was removed by evaporation. The silane@TiO_2 nanoparticles were washed with ethanol three times for the removal of physically adsorbed vinyltriethoxysilane. Finally, the silane@TiO_2 powder was dried at 110°C for 2 h in a oven. The schematic representation for the synthesis of silane@TiO_2 is summarized in scheme 1.

2.3 *General procedure for synthesis of benzo[4,5] imidazo[1,2-a]chromeno[4,3-d]pyrimidin-6-one*

In a 50 mL round-bottom flask, a mixture of 4-hydroxycoumarin **1** (2 mmol, 0.32 g), aldehyde **2a-q**

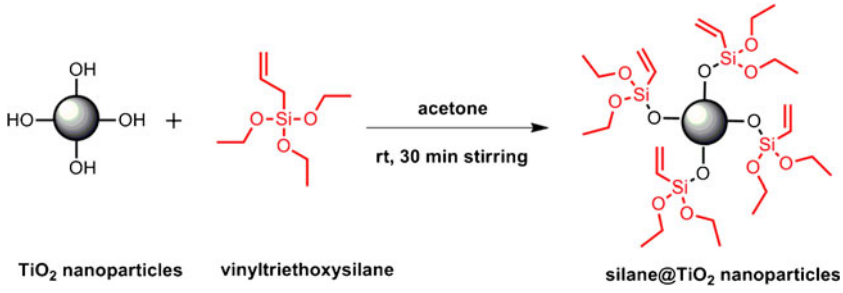

Scheme 1. Schematic route for the synthesis of the silane@TiO_2 nanoparticles.

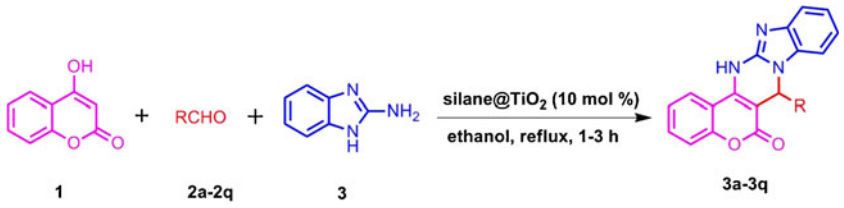

Scheme 2. Synthesis of benzo[4,5]imidazo[1,2-a]chromeno[4,3-d]pyrimidin-6-one using silane@TiO_2 nanoparticles.

(2 mmol), 2-aminobenzimidazole **3** (2 mmol, 0.27 g) and 10 mol% of silane@TiO_2 catalyst in ethanol (5 mL) was heated at reflux for specified time (table 3). After completion of the reaction (monitored by TLC), the reaction mixture was filtered and then the solid residue was dissolved in DMF (5 mL), followed by centrifugation of the mixture for 5–10 min at 2000–3000 rpm to remove the catalyst. The organic solution was then poured into cold water (15 mL), filtered, washed with ethanol and dried to afford the pure products. (The residual catalyst was washed with ethanol and dried in oven at 110°C for 2–3 h and reused) (scheme 2).

2.4 *DPPH free radical scavenging assay*

The scavenging of α,α-diphenyl-β-picrylhydrazyl (DPPH) radical by chemically synthesized seventeen compounds were analysed. One millilitre of 0.2 mM DPPH reagent prepared in methanol were added in tubes containing 0.8 mL of each compound (1 mg mL^{-1} in DMSO) and the mixture was allowed to stand for 30 min in the dark at room temperature. Similarly, same protocol was performed for L-ascorbic acid as a standard antioxidant. The absorbance of the resulting mixture was measured at 517 nm using UV-Vis spectrophotometer. The control was prepared by adding only DMSO to DPPH reagent and the analysis followed as described above. The % scavenging activity was determined as follows.

$$\text{Radical scavenging activity } (\%) = [(A_0 - A_1)] / A_0 \times 100$$

Where, A_0 is the absorption of the control (blank, only DMSO) and A_1 is the absorption of the compound.

3. Results and Discussion

3.1 *FT-IR analysis of the catalyst*

The surface modification of TiO_2 nanoparticles was evaluated by FT-IR spectroscopy. The figure 1 shows the FT-IR spectrum of TiO_2 (a), silane@TiO_2 (b) and vinyltriethoxysilane (c). In the spectrum 1a, the hydroxyl groups present on the surface of nano TiO_2 exhibit absorption bands at 3348 and 3453 cm^{-1}, respectively, which were found to be absent in the spectrum 1b. This indicates the absence of hydroxyl groups on the surface of silane@TiO_2, as ethoxy groups of vinyltriethoxy silane get condensed with hydroxyl groups present on TiO_2 surface. The bands at 1100 cm^{-1} and 760 cm^{-1} are assigned to the symmetrical and asymmetrical stretching of the Si-O bonds, respectively. The bands appearing at 1400 cm^{-1} also substantiate the presence of Si-C bond of vinyltriethoxy silane. The absorption band at 2990 cm^{-1} is attributed to symmetrical and asymmetrical stretchings of $-CH_2$ and $-CH_3$ groups. Thus, FT-IR spectra confirm the successful surface modification of TiO_2 nanoparticles.

3.2 *XRD spectral analysis*

Figure 2 shows the XRD patterns of TiO_2 and silane@TiO_2 nanoparticles. The peaks appearing at 101, 111, 112, 210, 121, 212, 032, 114, 024 are for the crystalline portion of TiO_2. The patterns allow the comparison with similar peaks that appeared in case of silane@TiO_2 compared to the TiO_2 nanoparticles, at 2θ values corresponding to the planes 101, 112, 200, 211, 204, 220, 301. Therefore, it is satisfying to observe

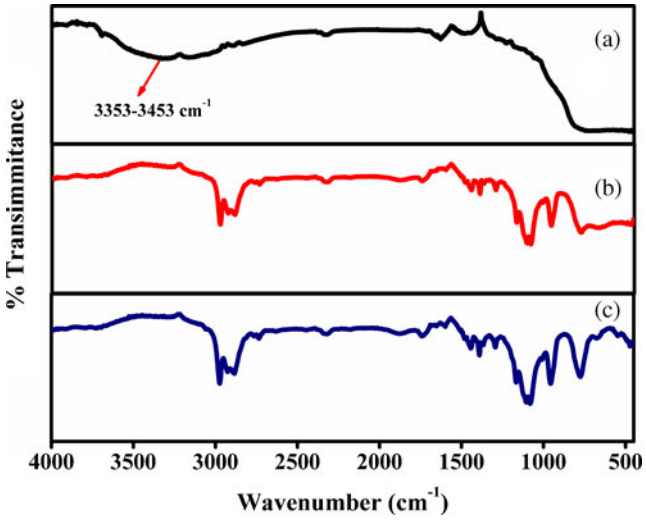

Figure 1. FT-IR spectra of (a) TiO_2, (b) silane@TiO_2, and (c) vinyltriethoxysilane.

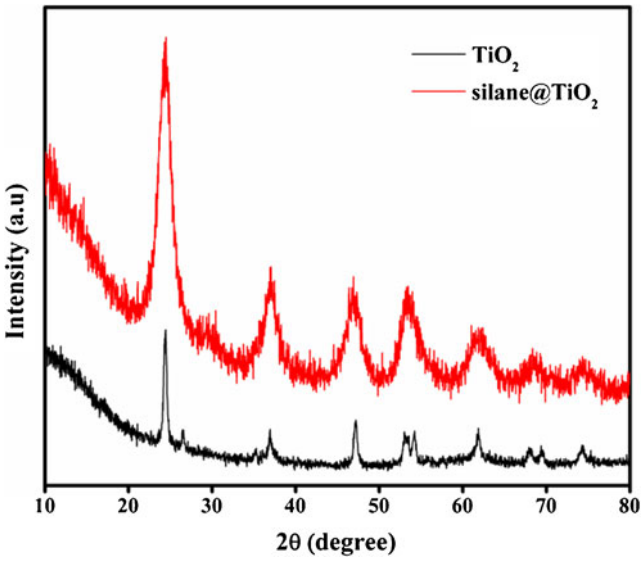

Figure 2. XRD pattern of TiO_2 and silane@TiO_2 nanoparticles.

that the modification of TiO_2 does not change the crystalline structure of silane@TiO_2. The XRD pattern of silane@TiO_2 shows broad peak at $2\theta = 15–25°$ which indicates the amorphous nature of silica.[29] The most intense peak of silane@TiO_2 nanoparticles was used to determine the size of crystallites to be approximately 5.4 nm, using the half-width of the diffraction peak and the Debye-Scherrer equation. The Sherrer's equation is $D = K\lambda/\beta\cos\theta$, where D is the crystallite size, λ is wavelength of the radiation, θ is the Bragg's angle and β is the full width at half maximum.

3.3 *FE-SEM and EDX analysis of the catalyst*

FE-SEM analysis is another useful tool for the analysis of the surface morphology of a catalyst. The FE-SEM images of TiO_2 and silane@TiO_2 nanoparticles are shown in figure 3 (a–b). Notably, the particles are seen to be in the nano range (<100 nm). Figure 3c shows the EDX spectrum of silane@TiO_2 nanoparticles in which the characteristic peaks of Si and C are observed, which confirm the conversion of TiO_2 into silane@TiO_2 nanoparticles.

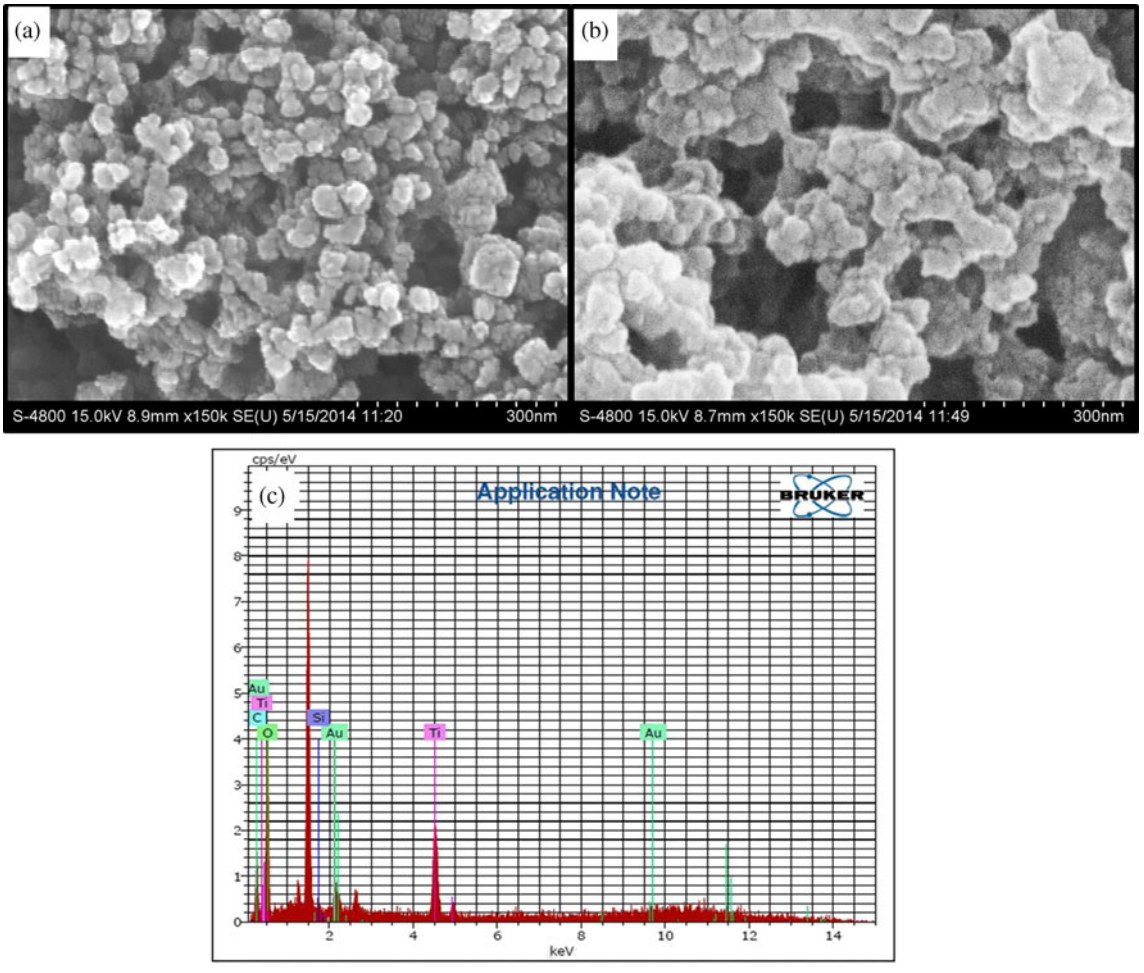

Figure 3. (a, b) FE-SEM images of TiO_2 and silane@TiO_2 nanoparticles, and (c) EDX spectrum of silane@TiO_2 nanoparticles.

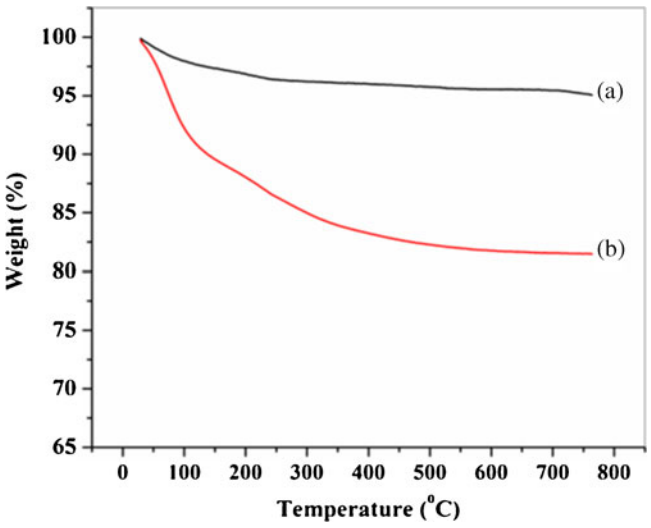

Figure 4. TGA thermograms of (a) TiO_2 and (b) silane@TiO_2 nanoparticles under nitrogen atmosphere at a heating rate of 10°C/min.

3.4 *TG analysis of the catalyst*

The thermal properties of TiO_2 and silane@TiO_2 nanoparticles were investigated using thermo gravimetric analysis (TGA) and the observed results are shown in figure 4. The TGA curve (a) shows slight weight loss (4.83%) probably due to vaporization of water or other volatile impurities that were physically adsorbed at the particle surface. The TiO_2 nanoparticles were relatively stable in air and somewhat decomposed. The TGA curve (b) shows two step degradation in that the first weight loss started from 28–165°C (10.69%) and second weight loss began in the range of 165–762°C (7.61%). The silane@TiO_2 nanoparticles showed two steps weight loss which is attributed to dehydration of the water absorbed by nanoparticles and oxidative thermal decomposition of the grafted vinyltriethoxy silane on the TiO_2 nanoparticles.

3.5 *TEM analysis*

The morphology of the nanoparticles of TiO_2 and silane@TiO_2 (figure 5a, b) was studied using transmission electron microscopy (TEM). From TEM images it is observed that the TiO_2 nanoparticles have spherical morphology with an average particle size of about 8 nm, while the silane@TiO_2 nanoparticles show

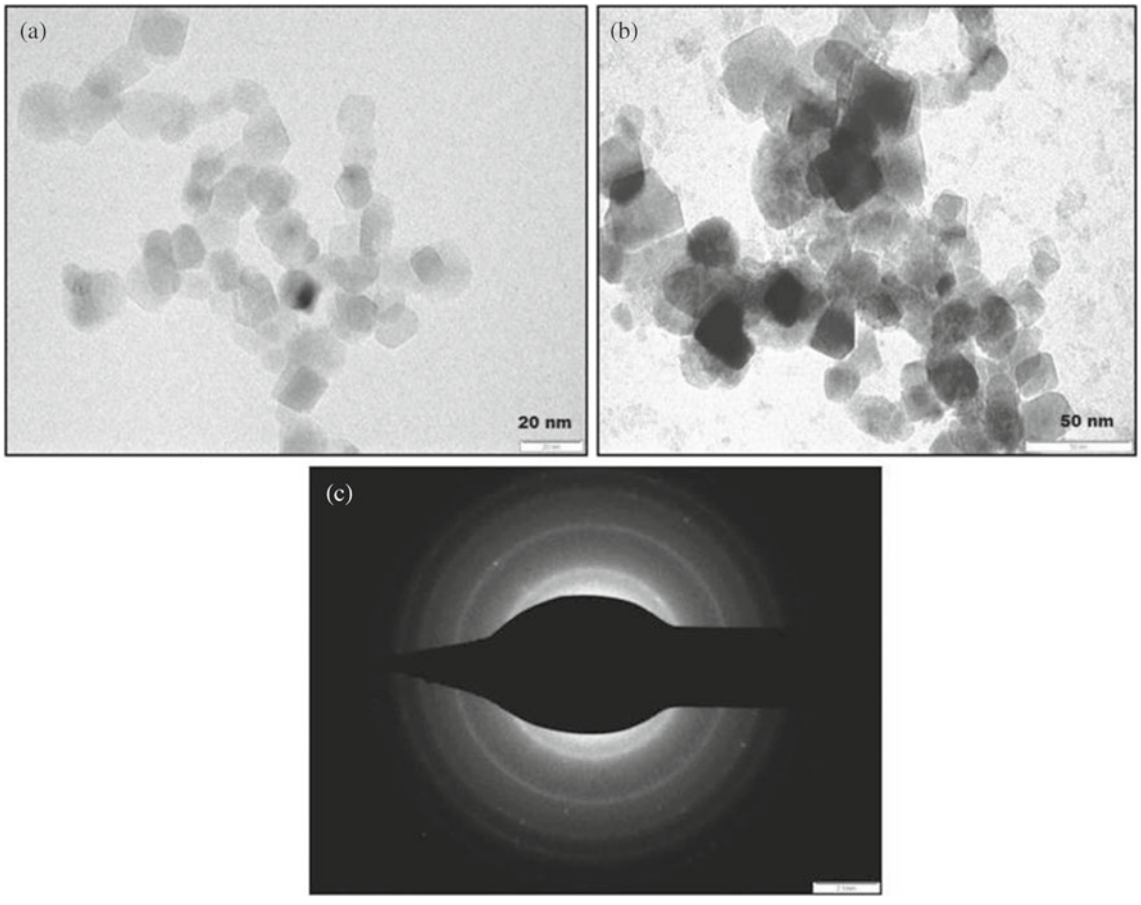

Figure 5. (a, b) TEM images TiO_2 and silane@TiO_2 nanoparticles. (c) Selected area electron diffraction pattern of silane@TiO_2 nanoparticles.

distorted spherical morphology with average particle size of about 9 nm. The TEM images thus indicate that the synthesized nanoparticles have nearly same crystalline character as that of TiO_2. The selected area electron diffraction (SAED) image of silane@TiO_2 nanoparticles (figure 5c) show ring patterns, confirming the crystalline nature.

3.6 *Optimization of reaction conditions*

We began our study from the reaction of 4-hydroxycoumarin **1** (2 mmol) with 3-nitrobenzaldehyde **2** (2 mmol), and 2-aminobenzimidazole **3** (2 mmol) as the model starting material in the presence of 5 mol% silane@TiO_2 nanoparticles in ethanol (5 mL) at 78–80°C for 1 h to give the desired product **3b** in 75% yield. Encouraged by this result, we further moved to study and optimize the best reaction conditions by using different amounts of silane@TiO_2 nanoparticles. The model reaction was stirred under same reaction conditions in the absence of silane@TiO_2 nanoparticles which yielded the target product **3b** in 33% yield only after 8 h (table 1, entry 1). Moreover, an increase in the amount (0 to 10 mol%) of silane@TiO_2 nanoparticles decreased the reaction time and increased the yield of the product (table 1, entries 1–4). However, the yield did not increase when excess amount (15 mol%) of silane@TiO_2 nanoparticles was used under similar reaction conditions. Therefore, 10 mol% of silane@TiO_2 nanoparticles was efficiently utilized for this multi-component reaction. Again, the model reaction was chosen for examining the effect of solvent on rate of reaction (table 2). The low yield of the target product **3b** was obtained when the mixture was refluxed for 6 h in the presence of 10 mol% of silane@TiO_2 nanoparticles in acetonitrile, toluene, THF, DMF, etc. (table 2, entries 1, 2, 3, 7). The reaction using ethanol as the solvent gave the corresponding product **3b** in high yield (81%) with short reaction time (table 2, entry 6). However, when the model reaction was carried at room temperature in ethanol (table 2, entry 5), even after 12 h only 30% yield was obtained. From these experimentations, it is clear that the reaction could not proceed smoothly at room temperature and hence refluxing under ethanol was preferred. Here, ethanol was chosen as the reaction medium for all further reactions since it is accepted as a green solvent. Therefore, the best and the most optimum reaction condition for the target reaction is 10 mol% of silane@TiO_2 nanoparticles as the catalyst in ethanol at reflux temperature. To study the recyclability and catalytic activity of the catalyst, the silane@TiO_2 nanoparticles (10 mol%) were used for the model reaction (table 1). The silane@TiO_2 nanoparticles can be recycled and reused as a catalyst for at least three times without significant loss in catalytic activity for this multi-component reaction (scheme 3).

To realize the efficiency and limitations of the catalyst in this multi-component reaction, we applied the optimized reaction conditions of 10 mol% silane@

Table 1. Effect of catalyst loading on the model reaction.[a]

Entry	Catalyst (mol %)	Time (h)	Yield of **3b**[b] (%)
1	0	8	33
2	5	1	75
3[c]	**10**	**1**	**81,79,75**
4	15	1	80

[a]Conditions: 4-hydroxycoumarin (2 mmol), 3-nitrobenzaldehyde (2 mmol), 2-aminobenzimidazole (2 mmol) and silane@TiO_2 nanoparticles (10 mol%), solvent (5 mL). [b]Isolated yields. [c]Catalyst was recycled for three times.

Table 2. Reaction of 4-hydroxycoumarin (**1**), 3-nitrobenzaldehyde (**2**), and 2 aminobenzimidazole (**3**) in different solvents.[a]

Entry	Solvent	Temp (°C)	Time (h)	Yield of **3b**[b] (%)
1	Acetonitrile	80	6	47
2	Toluene	100	6	36
3	THF	Reflux	6	40
4	Acetone	Reflux	2	60
5	Ethanol	RT	12	30
6	**Ethanol**	**78-80**	**1**	**81**
7	DMF	120	6	53
8	DCM	Reflux	5	46

[a]Conditions: 4-hydroxycoumarin (2 mmol), 3-nitrobenzaldehyde (2 mmol), 2-aminobenzimidazole (2 mmol), and silane@TiO_2 nanoparticles (10 mol%), solvent (5 mL). [b]Isolated yields.

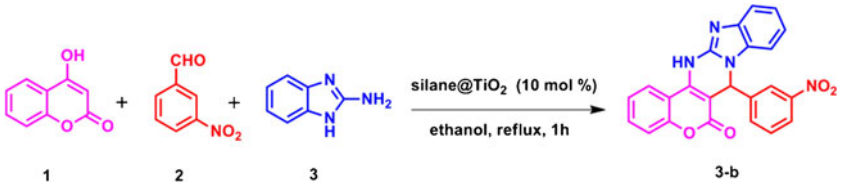

Scheme 3. Reaction of 4-hydroxycoumarin (**1**), 3-nitrobenzaldehyde (**2**), and 2-aminobenzimidazole (**3**) in the presence of silane@TiO_2 nanoparticles.

TiO_2 nanoparticles in ethanol at reflux temperature to a series of aldehydes (table 3). The aromatic and hetero-aromatic aldehydes could react smoothly to give the corresponding benzo[4,5]imidazo[1,2-a]chromeno [4,3-d]pyrimidin-6-one in good yields (table 3, entries 1–17). Most significantly, aromatic aldehydes carrying either electron-donating or electron-withdrawing substituents including hydroxyl group and methoxy group could react efficiently to give the corresponding products.

Herein, we propose a mechanism for the synthesis of benzo[4,5]imidazo[1,2-a]chromeno[4,3-d]pyrimidin-6-one (figure 6). It is assumed that silane@TiO_2 nanoparticles activate the carbonyl carbon of aldehyde through hydrogen bonding and promotes the Knoevenagel condensation reaction between 4-hydroxycoumarin

Table 3. Synthesis of benzo[4,5]imidazo[1,2-a]chromeno[4,3-d]pyrimidin-6-one using silane@TiO_2 nanoparticles.[a]

Entry	Ar	Product	Time (h)	Yield (%)[c]	M.p. (°C)
1	2-NO_2-C_6H_4	**3a**	1	75	230–232
2	3-NO_2-C_6H_4	**3b**	1	81	246–248
3	4-NO_2-C_6H_4	**3c**	1	82	208–210
4	2-Pyridinyl	**3d**	2	90	228–230
5	3-Pyridinyl	**3e**	2	83	>250 (dec.)
6	4-OCH_3-C_6H_4	**3f**	2	70	180
7	4-CH_3-C_6H_4	**3g**	2	90	202–204
8	4-Cl-C_6H_4	**3h**	2	91	218–220
9	3,4-$(OCH_3)_2$-C_6H_3	**3i**	1	91	180
10	4-F-C_6H_4	**3j**	1	91	230–232
11	3-Cl-C_6H_4	**3k**	1	86	238–240
12	3-OH-C_6H_4	**3l**	2	85	>250 (dec.)
13	4-OH-C_6H_4	**3m**	2	89	246–248
14	4-OH, 3,5-$(OCH_3)_2$-C_6H_2	**3n**	3	75	208–210
15	3-OH, 4-OCH_3-C_6H_3	**3o**	2	71	182–184
16	1-Naphthyl	**3p**	3	96	234–236
17	4-OH, 3-OCH_3-C_6H_3	**3q**	2	89	166–168

[a]General reaction conditions: 4-hydroxycoumarin **1** (2 mmol), aldehydes **2a-2q** (2 mmol), 2-aminobenzimidazole **3** (2 mmol), and silane@TiO_2 nanoparticles (10 mol%), ethanol (5 mL). [b]All products were characterized by IR, ^1H and ^{13}C NMR and mass spectrometry. [c]Isolated yield

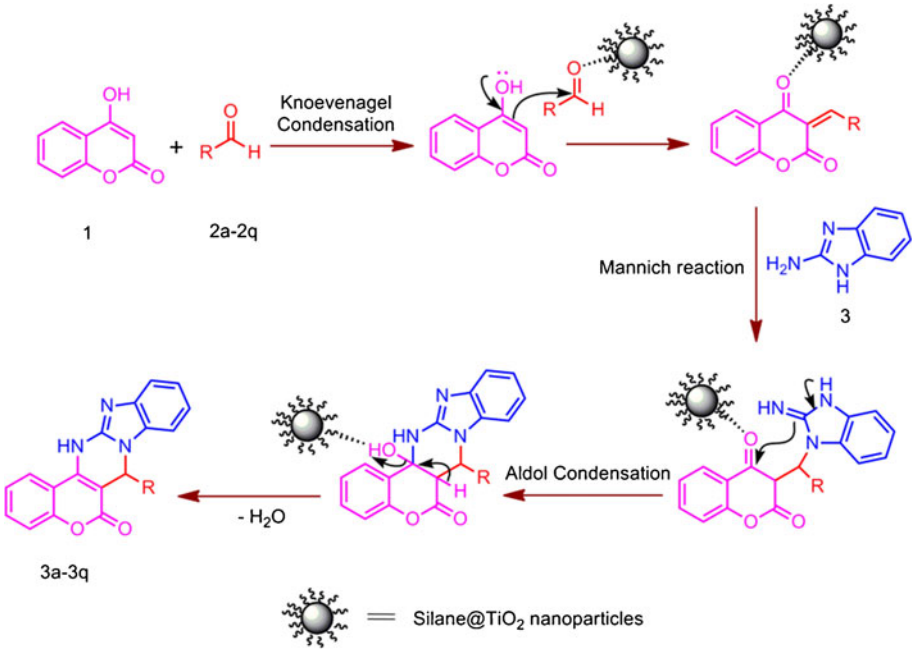

Figure 6. Plausible mechanism for the synthesis of benzo[4,5]imidazo[1,2-a]chromeno[4,3-d]pyrimidin-6-one.

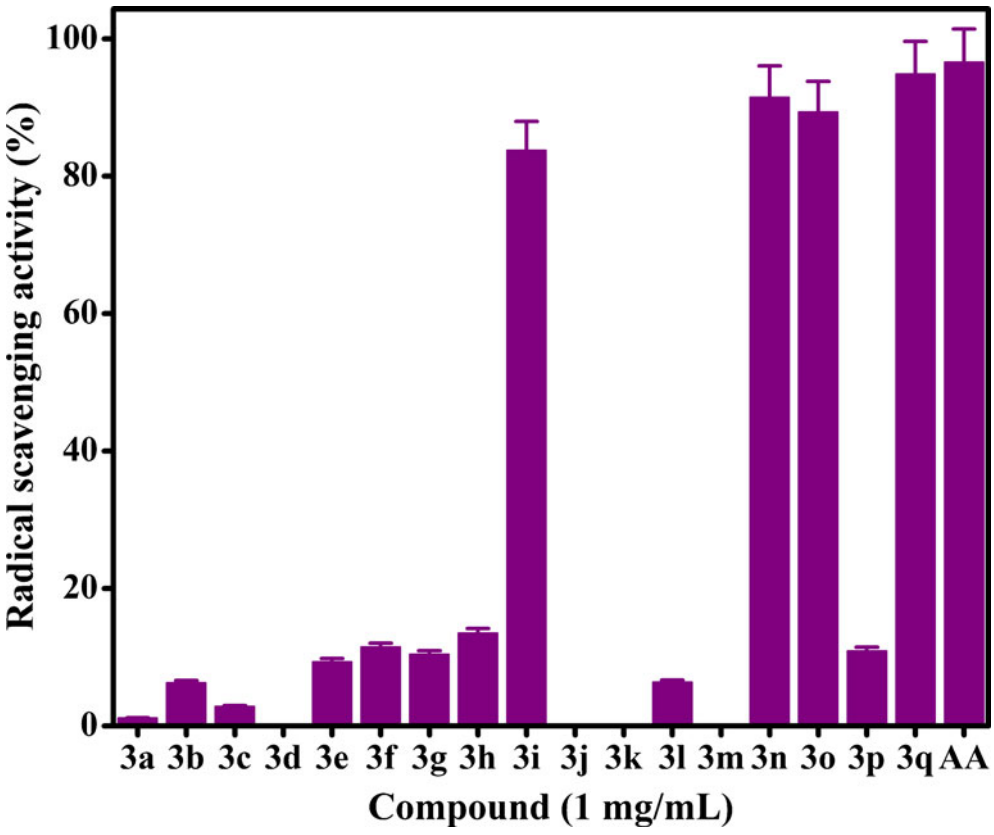

Figure 7. DPPH radical scavenging assay of synthesized compounds (**3a-3q**) and ascorbic acid (standard where AA= Ascorbic acid).

(**1**) and benzaldehyde (**2**) to form Schiff's base as an intermediate. In the next step, 2-aminobenzimidazole (**3**) reacts with the intermediate through Michael addition followed by cyclization and dehydration, to give the corresponding desired products.

3.7 *Biological evaluation*

3.7a *DPPH Radical scavenging assay*: Antioxidant activity of compounds is related to their electron or hydrogen atom donating ability to DPPH radical, so that they become stable diamagnetic molecules. The DPPH is a stable free radical and it accepts an electron or hydrogen atom to become a stable diamagnetic molecule.[30] The reduction competency of DPPH radicals was determined by a decrease in their absorbance at 517 nm induced by antioxidants. The absorption maximum of a stable DPPH radical in methanol was at 517 nm. The decrease in absorbance of DPPH radical was caused by antioxidants because of the reaction between antioxidant molecules and radical, which resulted in the scavenging of the DPPH radicals.

The electronic absorption spectra of solutions of compounds (**3a-q**) were measured in DMSO. All the synthesized compounds were screened for their antioxidant activity by measuring their scavenging ability towards DPPH radical. The disappearance of DPPH was measured spectrophotometrically at 517 nm using ascorbic acid as standard. The results are shown in figure 7. It can be concluded from figure 7 that four compounds **3i**, **3n**, **3o** and **3q** showed radical scavenging activity comparable to the standard ascorbic acid, whereas other compounds **3b**, **3e**, **3f**, **3g**, **3h**, **3l** and **3p** showed lower scavenging activity.

4. Conclusion

In summary, we have developed an efficient and environmentally benign method for the synthesis of benzo[4,5]imidazo[1,2-a]chromeno[4,3-d]pyrimidin-6-one using silane@TiO_2 nanoparticles as heterogeneous catalyst. The method has advantages such as clean and mild reaction conditions, short reaction time and excellent yield of products. Further, it is noteworthy to mention that, amongst the synthesized compounds, four compounds showed antioxidant activity comparable to ascorbic acid. The present work adheres to the concept of green chemistry and provides a synthetic strategy for chemists to opt for and confront research on multi-component reactions *via* use of nanocatalysts.

Supplementary Information (SI)

Spectral data, ^{1}H and ^{13}C NMR Spectra and Mas spectra are shown in Supplementary Information, available at www.ias.ac.in/chemsci.

Acknowledgements

Authors are thankful to UGC, New Delhi for financial assistance under One Time Grant [F. No. 19-110/2013 (BSR)] and Major Research Project [F. No. 41-302/2012 (SR)]; Authors also thankful to SAIF, Panjab University, Chandigarh, SAIF IIT Bombay and Central Instrumentation Facility Centre, UICT, NMU, Jalgaon for providing instrumental facilities.

References

1. (a) Gawande M B, Bonifacio V D B, Varma R S, Nogueira I D, Bundaleski N, Ghumman C A A, Teodoro O M N D and Branco P S 2013 *Green Chem.* **15** 1226; (b) Khedkar M V, Shinde A R, Sasaki T and Bhanage B M 2014 *J. Mol. Catal. A: Chem.* **385** 91; (c) Santra S, Rahman M, Roy A, Majee A and Hajra A 2014 *Catal. Commun.* **49** 52; (d) Naeimi H and Nazifi Z S 2014 *Appl. Catal. A* **477** 132
2. Mallakpour S and Nikkhoo E 2014 *Adv. Powder Technol.* **25** 348
3. Zhao J, Milanova M, Warmoeskerken M M C G and Dutschk V 2012 *Colloids Surf. A: Physicochem. Eng. Aspects* **413** 273
4. Zamani F, Hosseini S M and Kianpour S 2013 *Solid State Sci.* **26** 139
5. Tomovska R, Daniloska V and Asua J M 2013 *Appl. Surf. Sci.* **264** 670
6. Chen X and Mao S S 2007 *Chem. Rev.* **107** 2891
7. Mohammadi R and Kassaee M Z 2013 *J. Mol. Catal. A: Chem.* **380** 152
8. Yin Z F, Wu L, Yang H G and Su Y H 2013 *Phys. Chem. Chem. Phys.* **15** 4844
9. (a) Gupta S M and Tripathi M 2011 *Chin. Sci. Bull.* **56** 1639; (b) Ismail A A and Bahnemann D W 2011 *J. Mater. Chem.* **21** 1686
10. Ramon D J and Yus M 2005 *Angew. Chem. Int. Ed.* **44** 1602
11. Volla C M R, Atodiresei I and Rueping M 2014 *Chem. Rev.* **114** 2390
12. Tietze L F 1996 *Chem. Rev.* **96** 115
13. (a) Singh M S and Chowdhury S 2012 *RSC Adv.* **2** 4547; (b) Reddy M V, Reddy G C S and Jeong Y T 2014 *RSC Adv.* **4** 24089; (c) Reddy M V, Rani C R and Jeong Y T 2014 *Tetrahedron* **70** 3762
14. Gu Y 2012 *Green Chem.* **14** 2091
15. Anastas P T, Warner J C 1998 In *Green Chemistry: Theory and practice* (Oxford University Press: Oxford UK)
16. Xiao Z, Lei M and Hu L 2011 *Tetrahedron Lett.* **52** 7099
17. Mahire V N and Mahulikar P P 2015 *Chin. Chem. Lett.* **26** 983
18. (a) Bansal Y and Silakari O 2012 *Bioorg. Med. Chem.* **20** 6208; (b) Shah N K, Shah N M, Patel M P and Patel RG 2013 *J. Chem. Sci.* **125** 525
19. (a) Richards M L, Lio S C, Sinha A, Tieu K K and Sircar J C 2004 *J. Med. Chem.* **47** 6451; (b) Craigo W A, LeSueur B W and Skibo E B 1999 *J. Med. Chem.* **42** 3324; (c) Raut C N, Bagul S M, Janrao R A, Vaidya S D, Kumar B V S and Mahulikar P P 2010 *J. Heterocycl. Chem.* **47** 582; (d) Raut C N, Bharambe S M, Pawar Y A and Mahulikar P P 2011 *J. Heterocycl. Chem.* **48** 419; (e) Kucukbaya H, Durmaz R, Okyucu N and Gunald S 2003 *Folia Microbiol.* **48** 679; (f) Kuş C, Ayhan-Kılcıgil G, Özbey S, Kaynak F B, Kaya M, Çoban T and Can-Eke B 2008 *Bioorg. Med. Chem.* **16** 4294; (g) Ansari K F and Lal C 2009 *J. Chem. Sci.* **121** 1017; (h) Kathrotiya H G and Patel M P 2013 *J. Chem. Sci.* **125** 993
20. Preston P N 1981 In *Benzimidazoles and congeneric tricyclic compounds* (Interscience and John Wiley: New York)
21. Jaggavarapu S R, Kamalakaran A S, Jalli V P, Gangisetty S K, Ganesh M R and Gaddamanugu G 2014 *J. Chem. Sci.* **126** 187
22. El-Agrody A M, Fouda A M and Al-Dies Al-A M 2014 *Med. Chem. Res.* **23** 3187
23. Kamdar N R, Haveliwala D D, Mistry P T and Patel S K 2011 *Med. Chem. Res.* **20** 854
24. Gupta J K, Sharma P K, Dudhe R, Chaudhary A, Singh A, Verma P K, Mondal S C, Yadav R K and Kashyap S 2012 *Med. Chem. Res.* **21** 1625
25. Dinakaran V S, Jacob D and Mathew J E 2012 *Med. Chem. Res.* **21** 3598
26. (a) Heravi M M, Saeedi M, Beheshtiha Y S and Oskooie H A 2011 *Chem. Heterocycl. Compd.* **47** 737; (b) Mazhukina O A, Platonova A G, Fedotova O V and Vasin V A 2015 *Russ. J. Org. Chem.* **51** 691
27. Mahshid S, Ghamsari M S, Askari M, Afshar N and Lahuti S 2006 *Semicond. Phys. Quant. Electro. Optoelectro.* **9** 65
28. (a) Sabzi M, Mirabedini S, Zohuriaan J and Atai M 2009 *Prog. Org. Coat.* **65** 222; (b) Gite V V, Chaudhari A B, Kulkarni R D and Hundiwale D G 2013 *Pigm. Resin Technol.* **42** 353; (c) Chaudhari A B, Gite V V, Rajput S D, Mahulikar P P and Kulkarni R D 2013 *Ind. Crop. Prod.* **50** 550
29. Dehghani F, Sardarian A R and Esmaeilpour M 2013 *J. Organomet. Chem.* **743** 87
30. Soarey J R, Dinis T C P, Cunha A P and Almeida L M 1997 *Free. Rad. Res.* **26** 469